Supplementary Information

Insights into Synergistic Effect of Active Centers over ZnMg/SBA-15 Catalyst in Direct Synthesis of Butadiene from Ethanol

Kangzhou Wang[a], Xiaobo Peng[a]*, Xinhua Gao[b], Yuya Araki[a], Heng Zhao[a], Jiaming Liang[a], Liwei Xiao[a], Jienan Chen[c], Guangbo Liu[d], Jinhu Wu[d], Guohui Yang[a]* and Noritatsu Tsubaki[a]*

[a]Department of Applied Chemistry, Graduate School of Engineering, University of Toyama, Gofuku 3190, Toyama 930-8555, Japan

[b]State Key Laboratory of High-efficiency Utilization of Coal and Green Chemical Engineering, Faculty of Chemistry and Chemical Engineering, Ningxia University, Yinchuan 750021, China

[c]Ministry of Forestry Bioethanol Research Center, School of Materials Science and Engineering, Central South University of Forestry and Technology, Changsha 410004, China

[d]Qingdao Institute of Biomass Energy and Bioprocess Technology, Chinese Academy of Science, Qingdao 266101, China

***Corresponding author**:

pengxb@eng.u-toyama.ac.jp (Xiaobo Peng)

thomas@eng.u-toyama.ac.jp (Guohui Yang)

tsubaki@eng.u-toyama.ac.jp (Noritatsu Tsubaki)

Table of contents

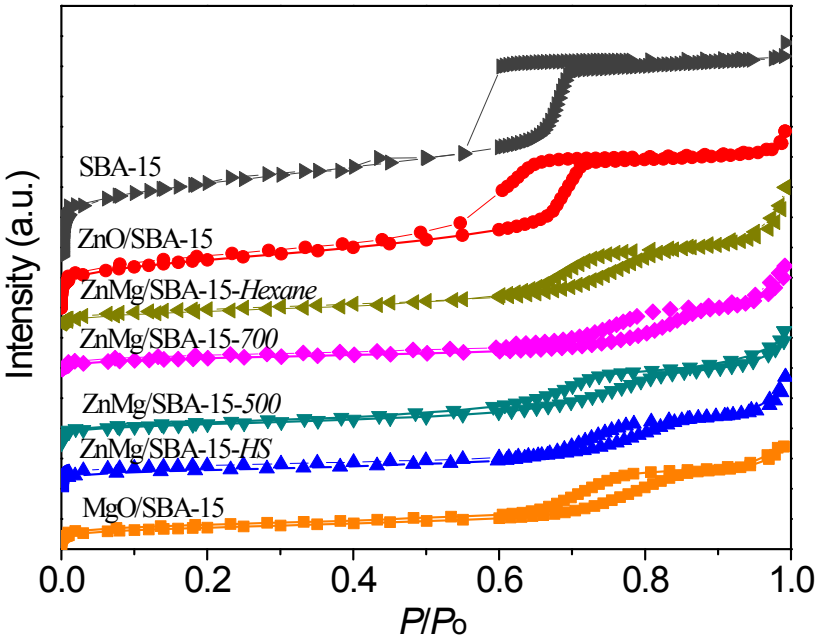

Fig. S1 N_2 adsorption-desorption isotherms for the SBA-15, ZnO/SBA-15, MgO/SBA-15 and ZnMg/SBA-15-based catalysts.

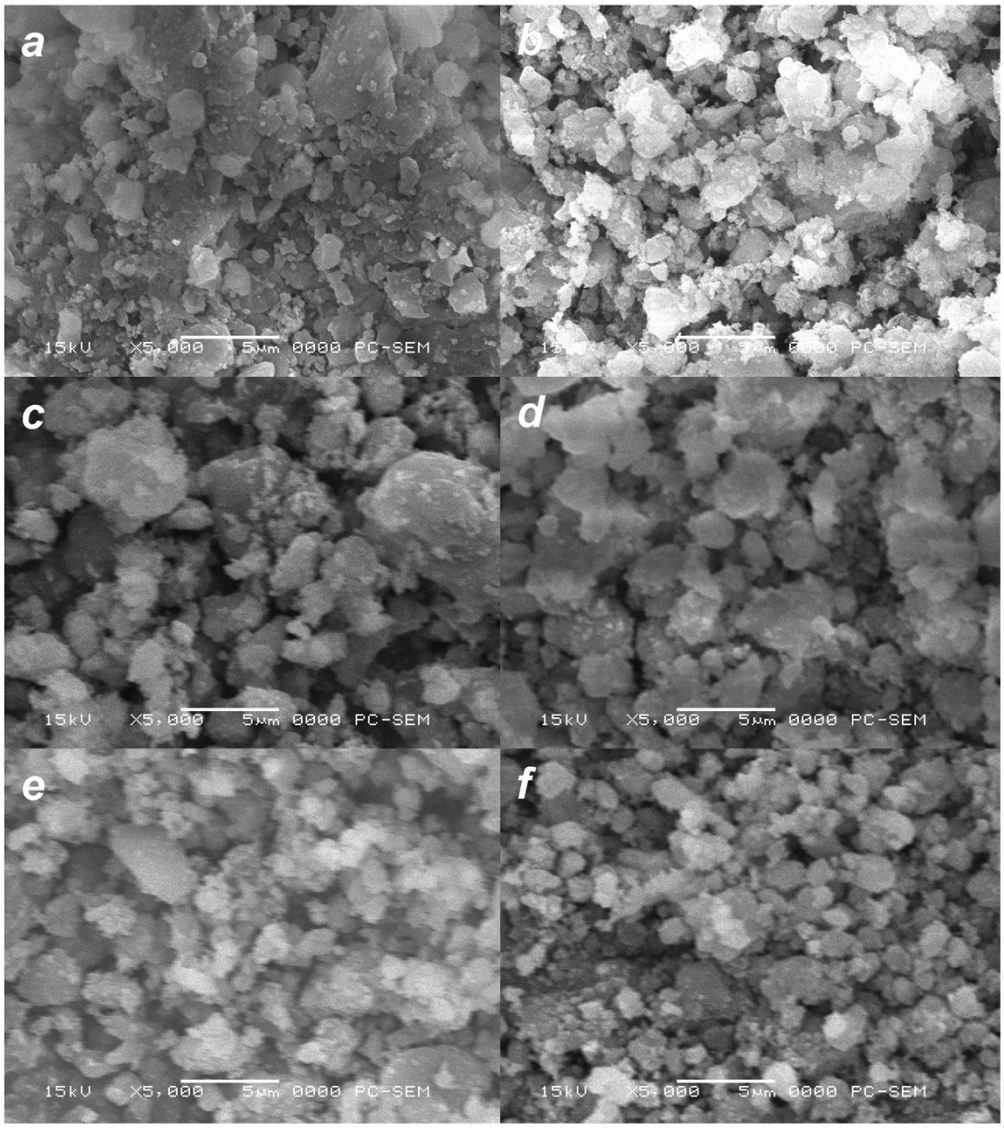

Fig. S2 SEM images of the MgO/SBA-15, ZnO/SBA-15 and ZnMg/SBA-15-based catalysts. (a) MgO/SBA-15, (b) ZnO/SBA-15, (c) ZnMg/SBA-15-*HS*, (d) ZnMg/SBA-15-*500*, (e) ZnMg/SBA-15-*700*, and (f) ZnMg/SBA-15-*Hexane*.

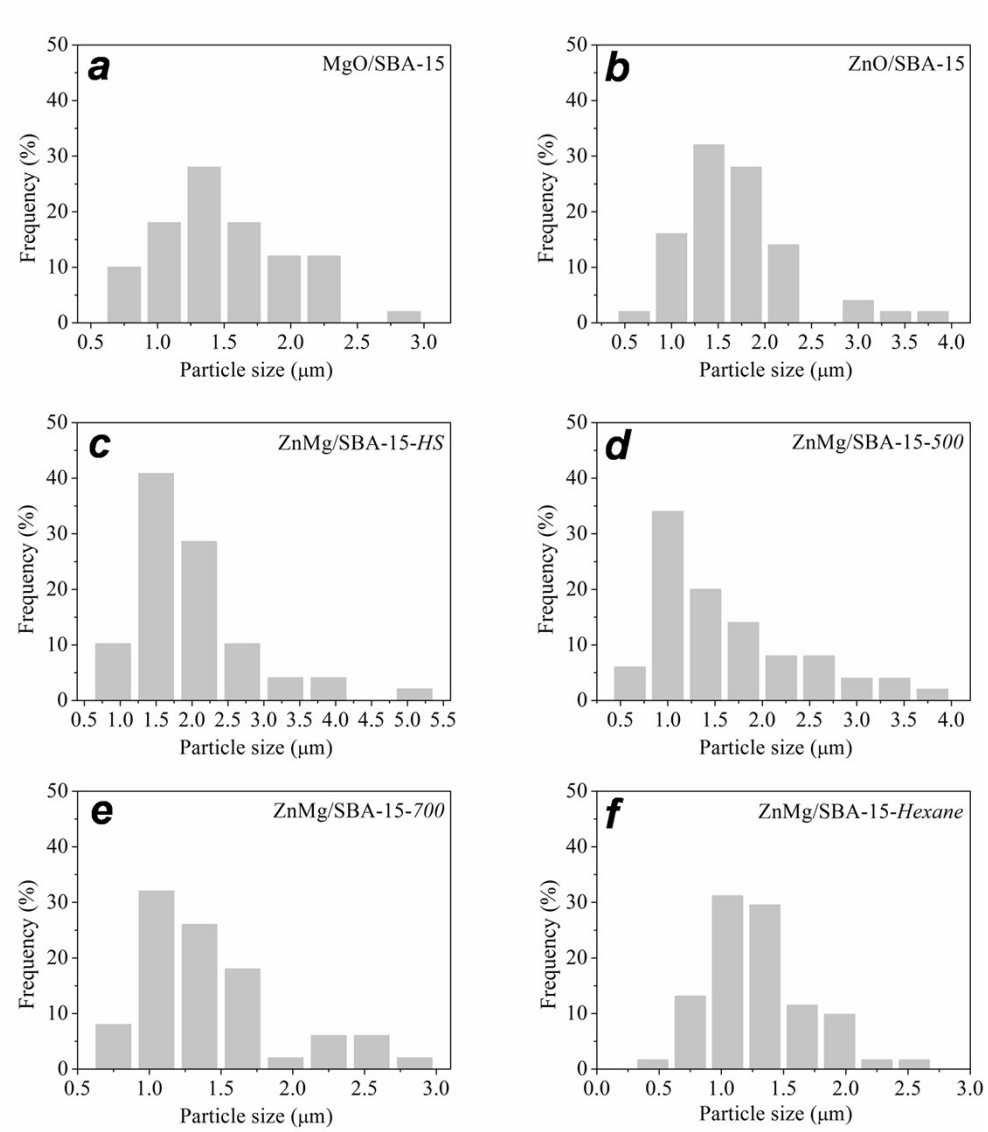

Fig. S3 Particle size distribution of the MgO/SBA-15, ZnO/SBA-15 and ZnMg/SBA-15-based catalysts. (a) MgO/SBA-15, (b) ZnO/SBA-15, (c) ZnMg/SBA-15-*HS*, (d) ZnMg/SBA-15-*500*, (e) ZnMg/SBA-15-*700*, and (f) ZnMg/SBA-15-*Hexane*. The average particle size was 1.51, 1.71, 1.98, 1.62, 1.42, and 1.30 μm for the MgO/SBA-15, ZnO/SBA-15, ZnMg/SBA-15-*HS*, ZnMg/SBA-15-*500*, ZnMg/SBA-15-*700*, and ZnMg/SBA-15-*Hexane*, respectively.

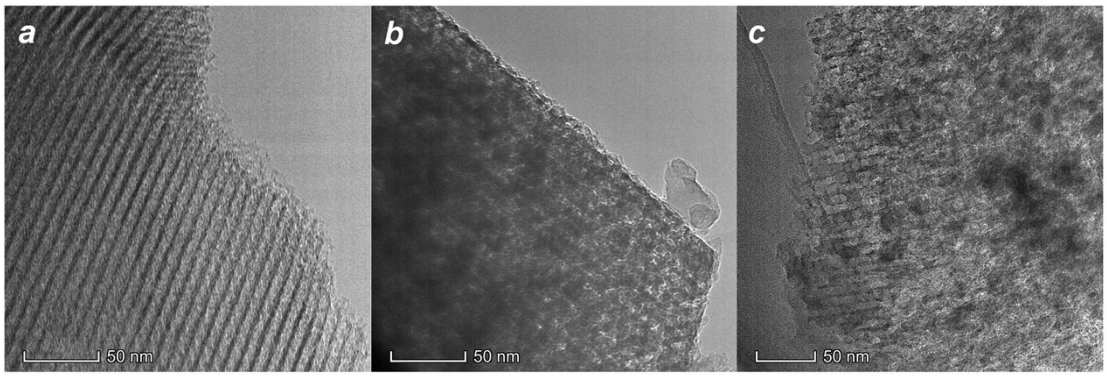

Fig. S4 TEM images of the catalysts of ZnO/SBA-15, MgO/SBA-15, ZnMg/SBA-15-*Hexane*. (a) ZnO/SBA-15, (b) MgO/SBA-15, and (c) ZnMg/SBA-15-*Hexane*.

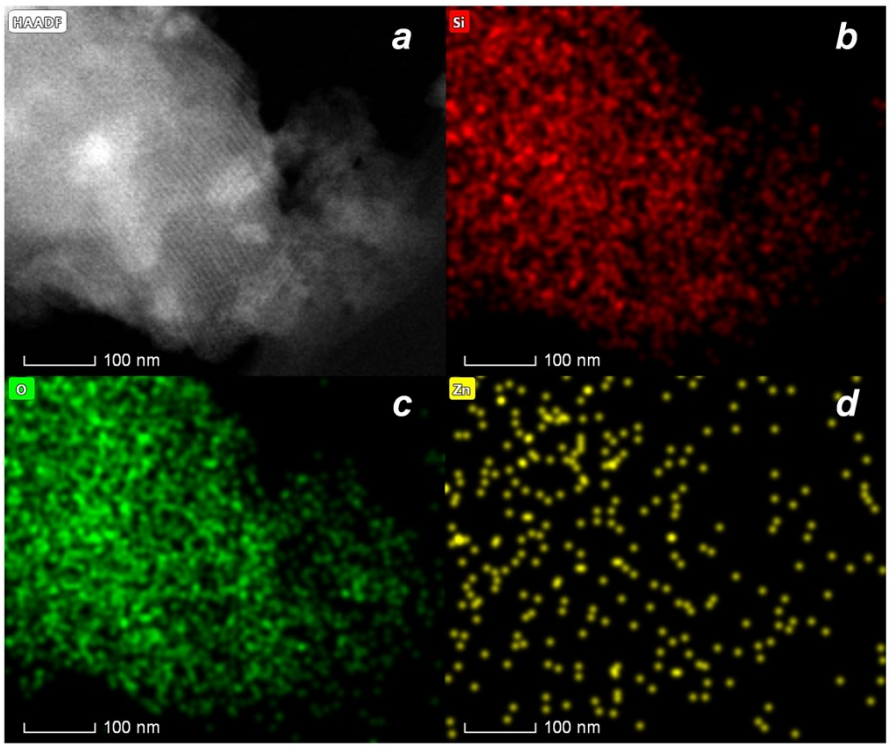

Fig. S5 Elemental mapping from STEM-EDS analysis for the ZnO/SBA-15 catalyst. (a) STEM image, (b) Si, (c) O, and (d) Zn.

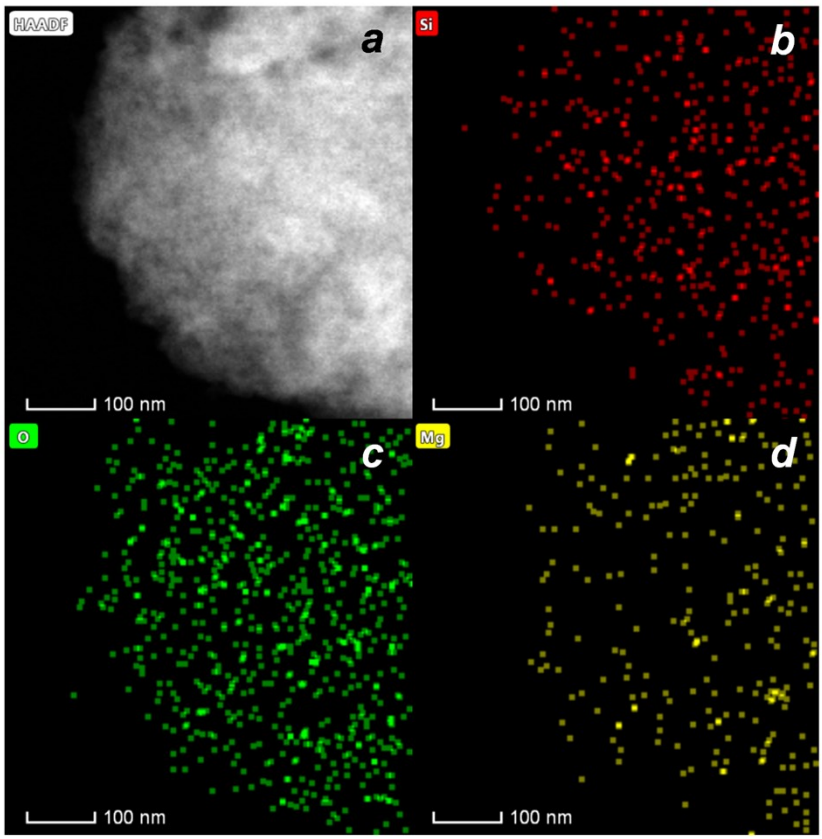

Fig. S6 Elemental mapping from STEM-EDS analysis for the MgO/SBA-15 catalyst. (a) STEM image, (b) Si, (c) O, and (d) Mg.

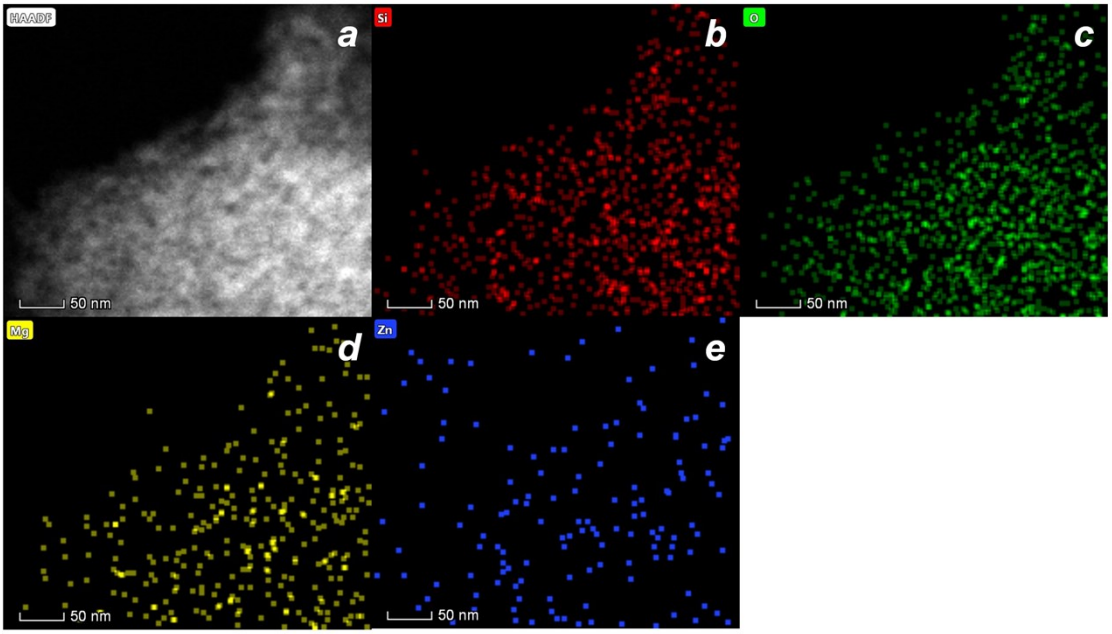

Fig. S7 Elemental mapping from STEM-EDS analysis for the ZnMg/SBA-15-*Hexane*. (a) STEM image, (b) Si, (c) O, (d) Mg, and (e) Zn.

Table S1 The elemental composition for the MgO/SBA-15, ZnO/SBA-15 and ZnMg/SBA-15-based catalysts.

Sample	Element content (wt%)[a]			Dosage of raw materials (wt%)[b]		
	Zn	Mg	Si	Zn	Mg	Si
MgO/SBA-15	/	41.7	58.3	/	46.2	53.8
ZnO/SBA-15	20.9	/	79.1	24.5	/	75.5
ZnMg/SBA-15-*HS*	7.6	40.2	52.2	16.6	43.0	40.4
ZnMg/SBA-15-*500*	8.2	41.5	50.3	7.5	42.7	49.7
ZnMg/SBA-15-*700*	8.8	40.5	50.7	7.5	42.7	49.7
ZnMg/SBA-15-*Hexane*	8.9	42.8	48.3	7.5	42.7	49.7

(a) The elemental composition of these catalysts was obtained by EDX analysis. (b) The dosages of the elements were calculated according to the amount of raw materials in the catalyst preparation.

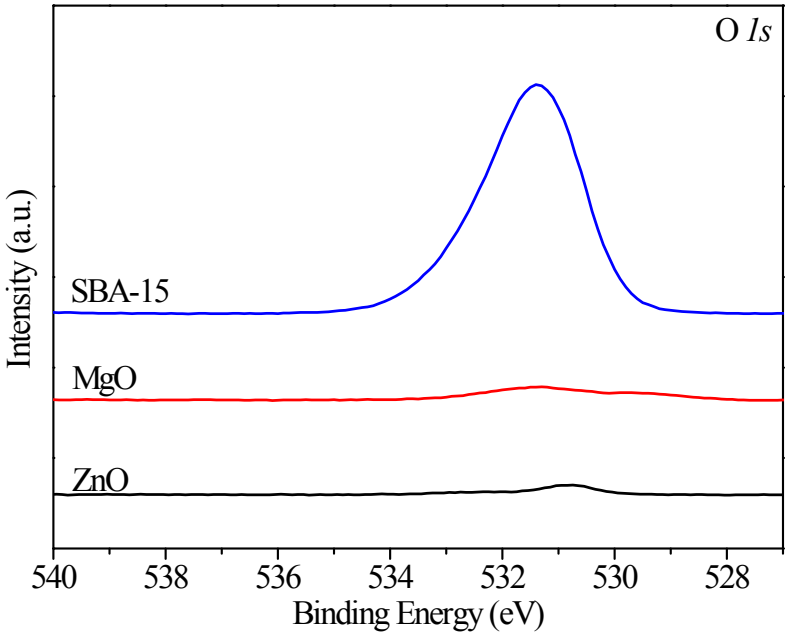

Fig. S8 Comparison of the O *1s* region on the ZnO, MgO, and SBA-15.

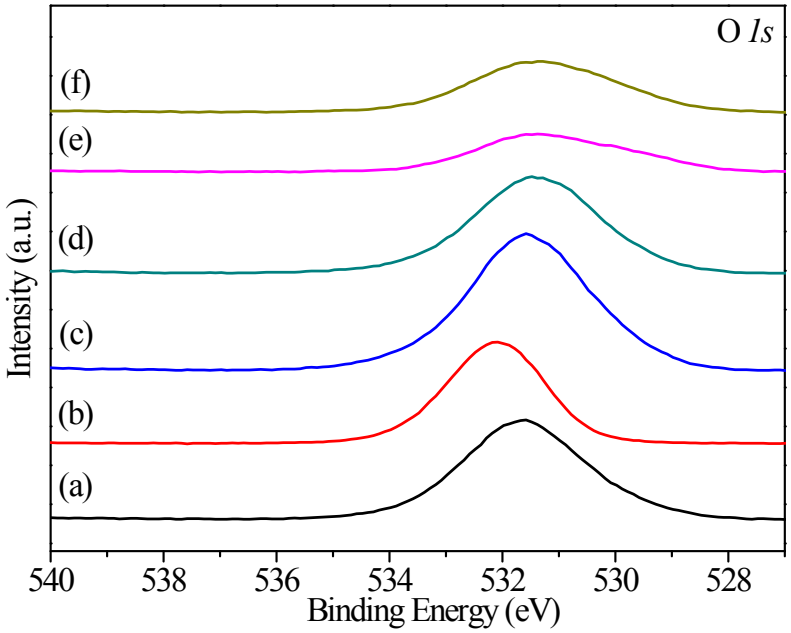

Fig. S9 O *1s* region for the MgO/SBA-15, ZnO/SBA-15 and ZnMg/SBA-15-based catalysts. (a) MgO/SBA-15, (b) ZnO/SBA-15, (c) ZnMg/SBA-15-*HS*, (d) ZnMg/SBA-15-*500*, (e) ZnMg/SBA-15-*700*, and (f) ZnMg/SBA-15-*Hexane*.

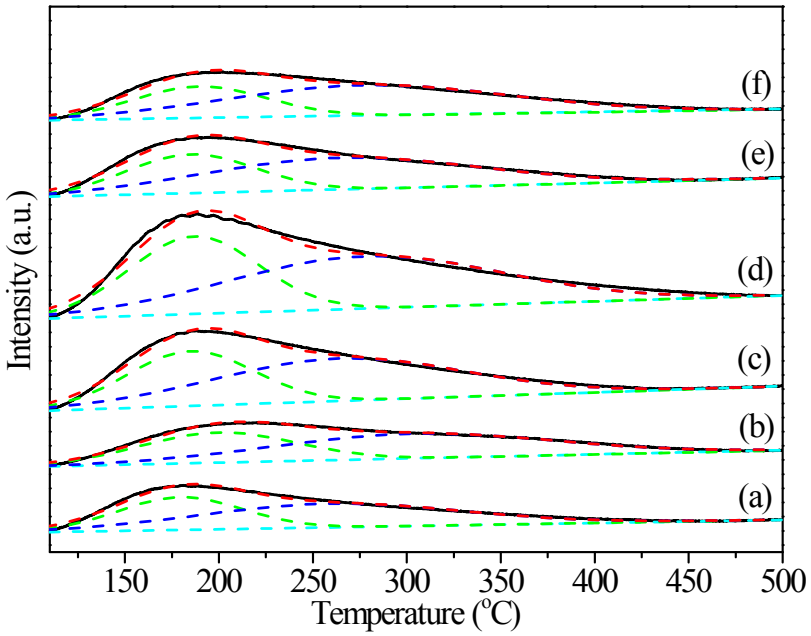

Fig. S10 NH_3-TPD profiles for the MgO/SBA-15, ZnO/SBA-15 and ZnMg/SBA-15-based catalysts. (a) MgO/SBA-15, (b) ZnO/SBA-15, (c) ZnMg/SBA-15-*HS*, (d) ZnMg/SBA-15-*500*, (e) ZnMg/SBA-15-*700*, and (f) ZnMg/SBA-15-*Hexane*.

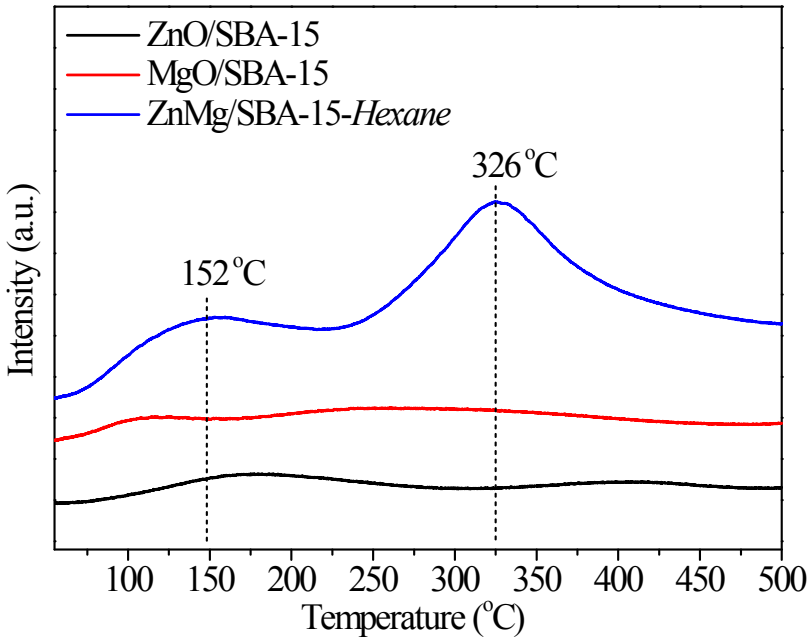

Fig. S11 CO_2-TPD profiles for the catalysts of ZnO/SBA-15, MgO/SBA-15 and ZnMg/SBA-15-*Hexane*.

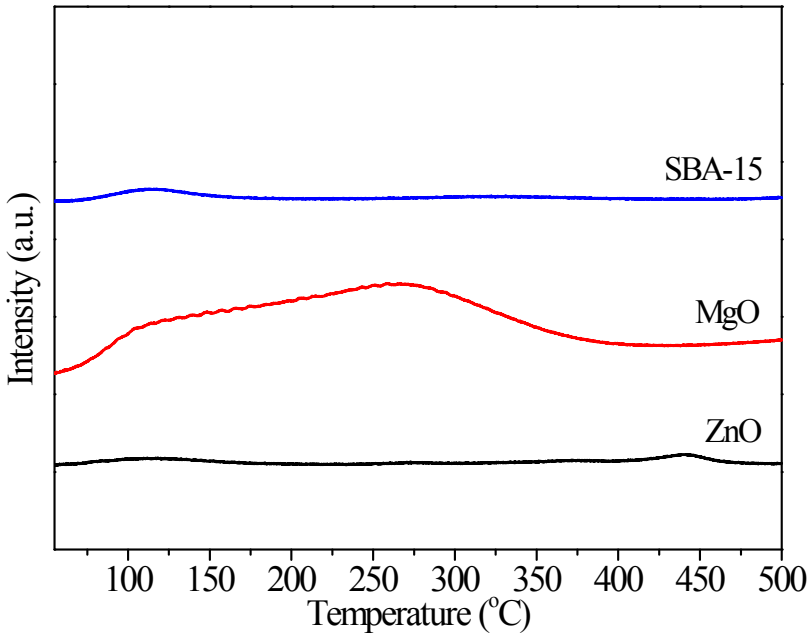

Fig. S12 CO_2-TPD analysis for the samples of ZnO, MgO, and SBA-15.

Table S2 Carbon balance for the MgO/SBA-15, ZnO/SBA-15 and ZnMg/SBA-15-based catalysts.

Sample	Carbon balance (%)
MgO/SBA-15	94.5
ZnO/SBA-15	84.3
ZnMg/SBA-15-HS	93.9
ZnMg/SBA-15-500	82.8
ZnMg/SBA-15-700	88.4
ZnMg/SBA-15-Hexane	93.4

The Carbon balance was calculated based on C-moles of the converted ethanol and the obtained products.

Table S3 Turnover rate for the MgO/SBA-15, ZnO/SBA-15 and ZnMg/SBA-15-based catalysts.

Sample	Turnover rate (h^{-1})
MgO/SBA-15	32.4
ZnO/SBA-15	75.0
ZnMg/SBA-15-*HS*	31.4
ZnMg/SBA-15-*500*	40.1
ZnMg/SBA-15-*700*	64.2
ZnMg/SBA-15-*Hexane*	88.2

The turnover rate was calculated according to the number of Lewis acid sites. In the direct ETB reaction, aldol condensation and MPV reaction were the rate-determining steps. Lewis acid sites were active Centers for the aldol condensation and MPV reaction. Therefore, we employed the number of Lewis acid sites to calculate the turnover rate of ethanol in the direct ETB processes.

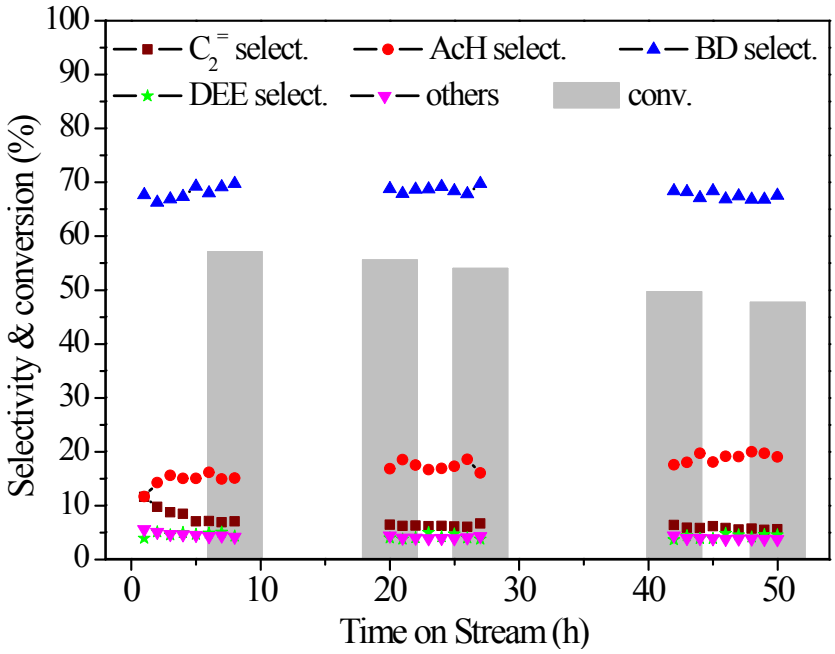

Fig. S13 Stability of the ZnMg/SBA-15-*Hexane* in direct ETB reaction. Reaction conditions: catalyst, 0.5 g; T = 400 °C; WHSV = 1.23 h^{-1}; TOS = 50 h. The ethylene, butadiene, acetaldehyde and diethyl ether was abbreviated as $C_2^=$, BD, AcH, and DEE, respectively.

Table S4 Performance comparison of the ZnMg/SBA-15-*Hexane* and other reported catalysts.[1,2]

Sample	Conversion (%)[a]	BD selectivity (%)[b]	BD productivity ($g_{BD}·g_{cat}^{-1}·h^{-1}$)[c]	Ref.
3.7%Ag/MgO(2)-SiO_2	97.7	63.0	0.07	1
4%ZnO/MgO-SiO_2	84.6	53.1	0.26	2
ZnMg/SBA-15-*Hexane*	57.0	70.0	0.29	This work

(a) Ethanol conversion (%), (b) butadiene selectivity (%), (c) butadiene productivity ($g_{BD}·g_{cat.}^{-1}·h^{-1}$).

Table S5 Direct ETB performance for the ZnMg/SBA-15-*Hexane* and ZnMg/SBA-15-*Hexane*-R.

Sample	Conversion (%)	Selectivity (%)					STY ($g \cdot g_{cat}^{-1} \cdot h^{-1}$)
		BD	$C_2^=$	AcH	DEE	others	
ZnMg/SBA-15-*Hexane*	57.0	70.0	7.0	12.6	4.8	5.6	0.29
ZnMg/SBA-15-*Hexane*-R	56.1	65.0	7.4	21.2	3.7	2.7	0.26

Reaction conditions: catalyst, 0.5 g; T = 400 °C; WHSV = 1.23 h^{-1}; TOS = 6 h.

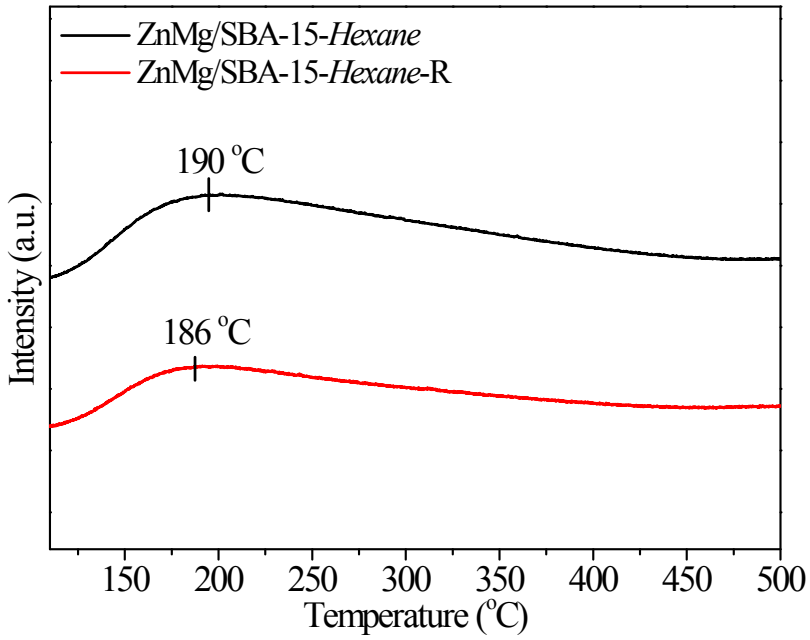

Fig. S14 NH_3-TPD analysis for the catalysts of ZnMg/SBA-15-*Hexane* and ZnMg/SBA-15-*Hexane*-R.

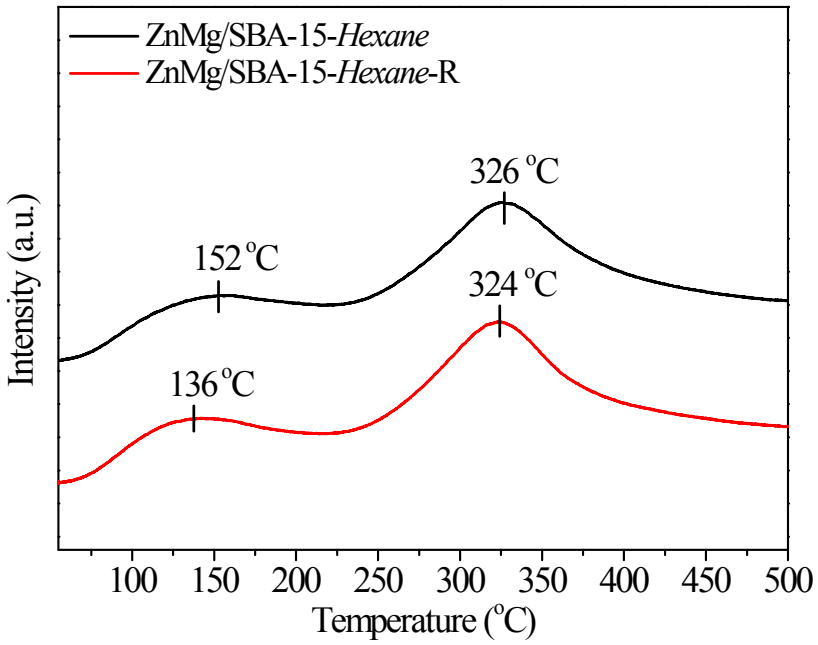

Fig. S15 CO_2-TPD analysis for the catalysts of ZnMg/SBA-15-*Hexane* and ZnMg/SBA-15-*Hexane*-R.

Table S6 Direct ETB performance for the ZnMg/SiO_2-*Hexane* and ZnMg/SBA-15-*Hexane*.

Sample	Conversion (%)	Selectivity (%)					STY ($g \cdot g_{cat}^{-1} \cdot h^{-1}$)
		BD	$C_2^=$	AcH	DEE	others	
ZnMg/SiO_2-*Hexane*	41.6	60.3	9.4	18.1	6.5	5.7	0.18
ZnMg/SBA-15-*Hexane*	57.0	70.0	7.0	12.6	4.8	5.6	0.29

Reaction conditions: catalyst, 0.5 g; T = 400 °C; WHSV = 1.23 h^{-1}; TOS = 6 h.

Table S7 Direct ETB performance for ZnO, MgO, and SBA-15.

Sample	Conversion (%)	Selectivity (%)					STY ($g \cdot g_{cat}^{-1} \cdot h^{-1}$)
		BD	$C_2^=$	AcH	DEE	others	
ZnO	63.2	0.4	27.7	28.4	23.0	20.5	0.00
MgO	11.5	3.3	38.3	52.6	1.6	4.1	< 0.01
SBA-15	3.8	0.0	53.6	22.7	16.8	7.7	0.00

Reaction conditions: catalyst, 0.5 g; T = 400 °C; WHSV = 1.23 h^{-1}; TOS = 6 h.

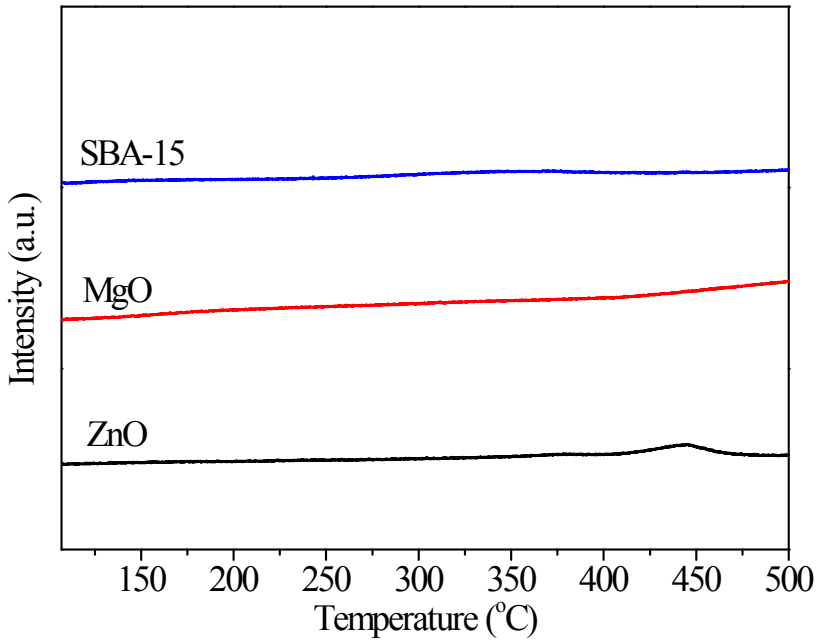

Fig. S16 NH_3-TPD analysis for the catalysts of ZnO, MgO, and SBA-15.

Table S8 Direct ETB performance over the ZnMg/SBA-15-*Hexane* catalysts with different ZnO contents.

Sample	Conversion (%)	Selectivity (%)					STY ($g \cdot g_{cat}^{-1} \cdot h^{-1}$)
		BD	$C_2^=$	AcH	DEE	others	
1ZnMg/SBA-15-Hexane	40.2	75.4	9.3	7.2	3.4	4.7	0.22
3ZnMg/SBA-15-Hexane	46.3	70.6	9.4	10.5	4.8	4.6	0.24
5ZnMg/SBA-15-Hexane	57.0	70.0	7.0	12.6	4.8	5.6	0.29
8ZnMg/SBA-15-Hexane	65.3	64.0	7.8	18.9	2.8	6.4	0.30
10ZnMg/SBA-15-Hexane	70.1	58.6	9.3	21.1	4.6	6.4	0.30

Reaction conditions: catalyst, 0.5 g; T = 400 °C; WHSV = 1.23 h^{-1}; TOS = 6 h.

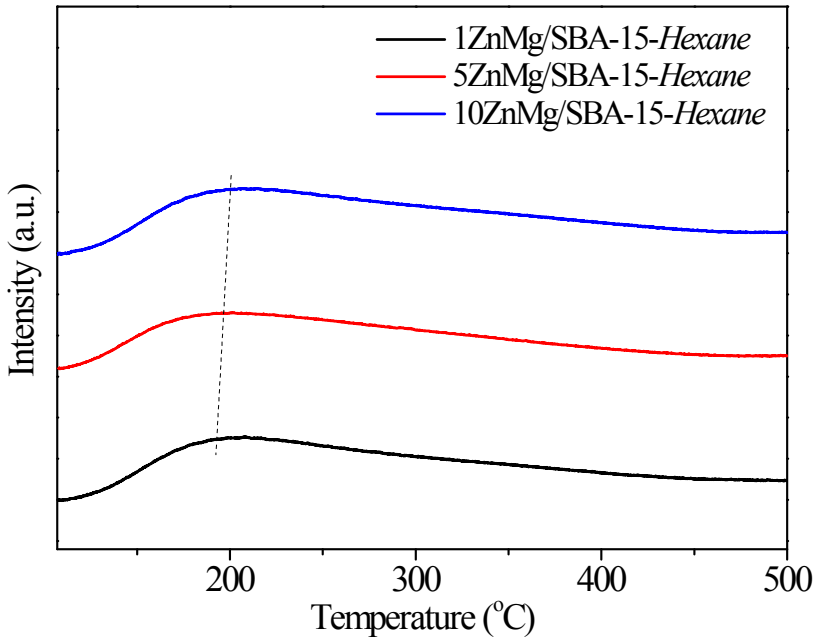

Fig. S17 NH_3-TPD analysis for the catalysts of 1ZnMg/SBA-15-*Hexane*, 5ZnMg/SBA-15-*Hexane* and 10ZnMg/SBA-15-*Hexane*.

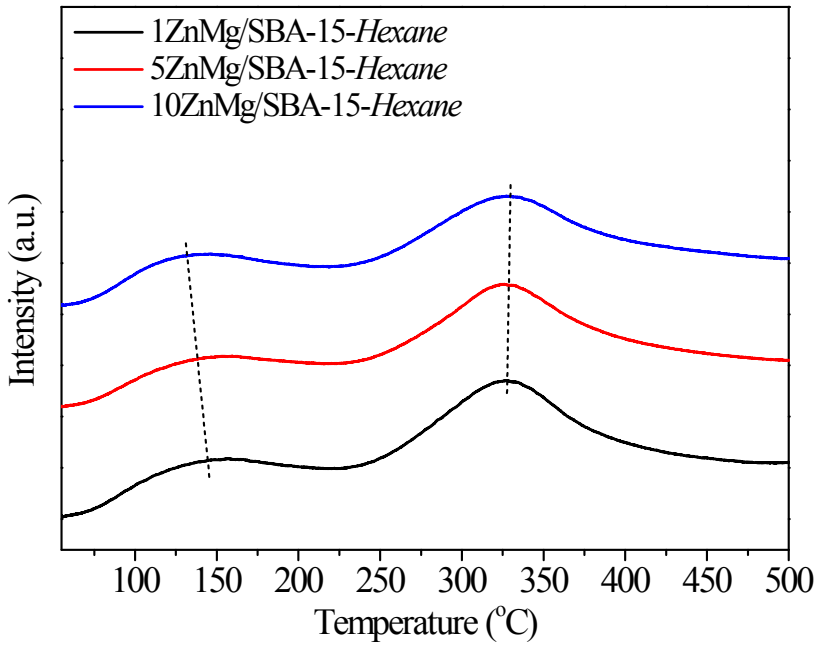

Fig. S18 CO_2-TPD analysis for the catalysts of 1ZnMg/SBA-15-*Hexane*, 5ZnMg/SBA-15-*Hexane* and 10ZnMg/SBA-15-*Hexane*.

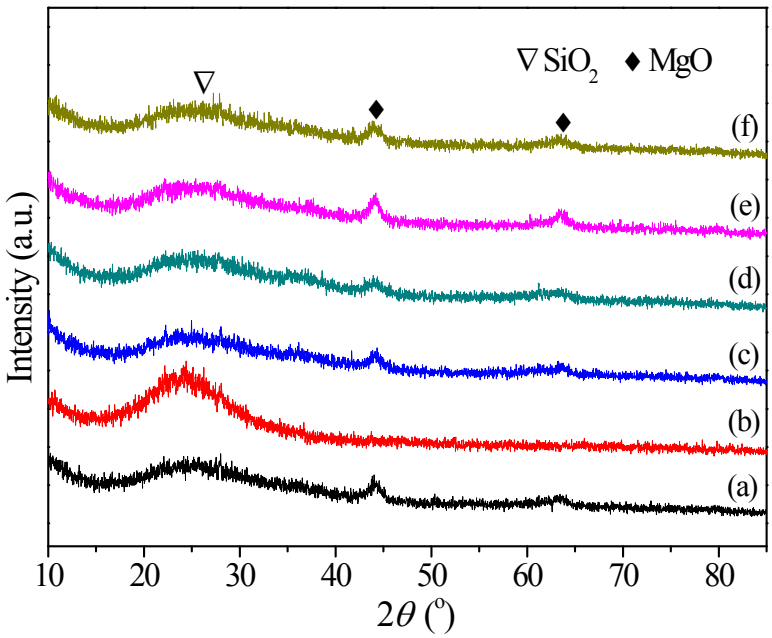

Fig. S19 XRD patterns for the spent MgO/SBA-15, ZnO/SBA-15 and ZnMg/SBA-15-based catalysts. (a) MgO/SBA-15, (b) ZnO/SBA-15, (c) ZnMg/SBA-15-*HS*, (d) ZnMg/SBA-15-*500*, (e) ZnMg/SBA-15-*700*, and (f) ZnMg/SBA-15-*Hexane*.

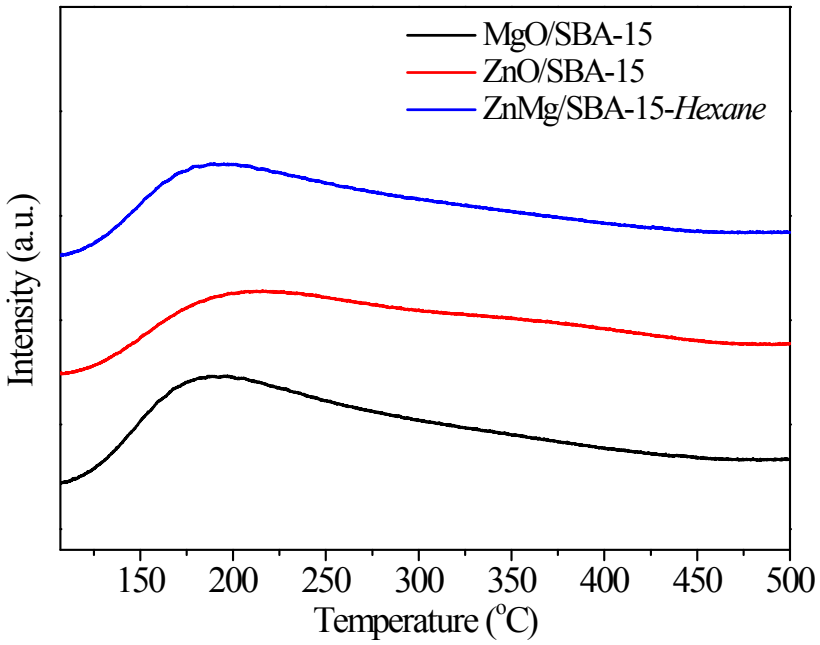

Fig. S20 NH_3-TPD profiles for the spent ZnO/SBA-15, MgO/SBA-15, and ZnMg/SBA-15-*Hexane*.

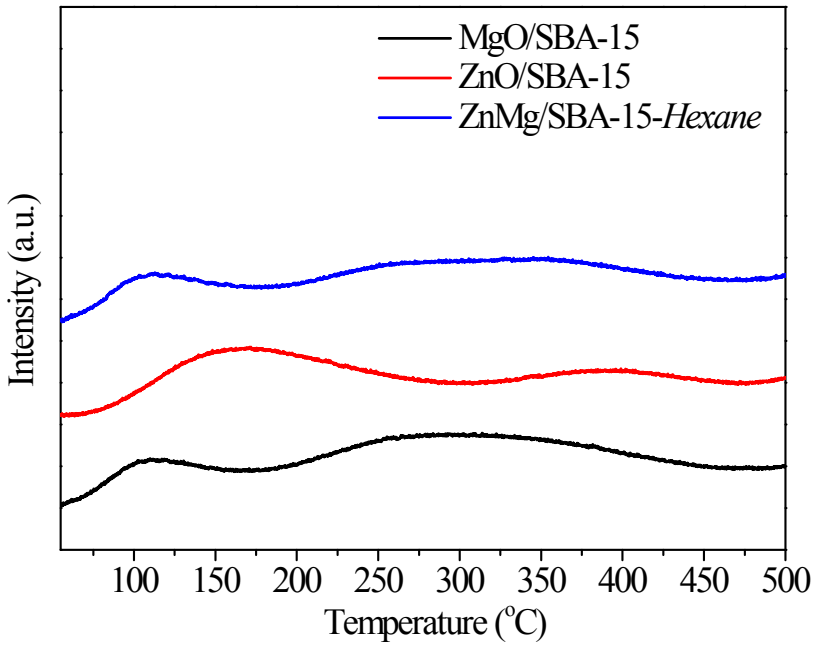

Fig. S21 CO_2-TPD profiles for the spent ZnO/SBA-15, MgO/SBA-15, and ZnMg/SBA-15-*Hexane*.

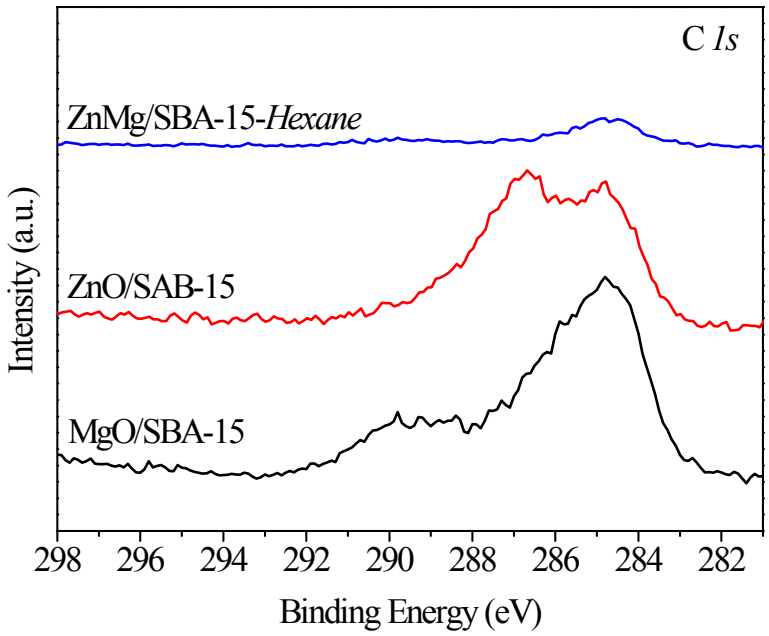

Fig. S22 C *1s* region for the spent MgO/SBA-15, ZnO/SBA-15, and ZnMg/SBA-15-*Hexane*.

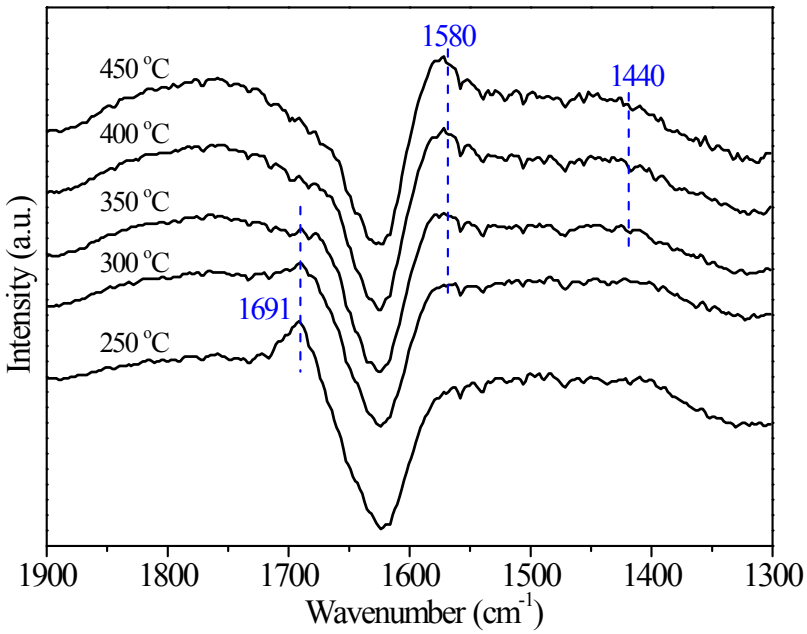

Fig. S23 *In-situ* DRIFT spectra for the direct ETB reaction from 250 to 450 °C over the ZnMg/SBA-15-*Hexane*.[3-6] The *In-situ* DRIFT spectra was showed using the frequency range from 1900 to 1300 cm^{-1}.

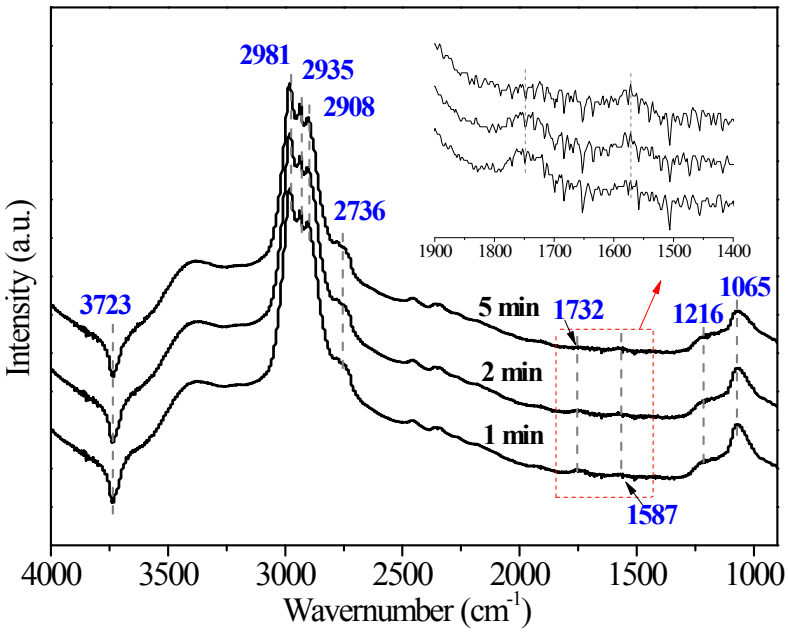

Fig. S24 *In-situ* DRIFT spectra for product desorption at 400 °C with He purge over the ZnO/SBA-15.[6] The inset further displayed the spectra for the frequency range from 1900 to 1400 cm^{-1}.

References

1. E. V. Makshina, W. Janssens, B. F. Sels, P. A. Jacobs, *Catal. Today*, 2012, **198**, 338-344.

2. O. V. Larina, P. I. Kyriienko, S. O. Soloviev, *Catal. Lett.*, 2015, **145**, 1162-1168.

3. Z. D. Young, S. Hanspal and R. J. Davis, *ACS Catal.*, 2016, **6**, 3193-3202.

4. J. V. Ochoa, C. Trevisanut, J. M. M. Millet, G. Busca and F. Cavani, *J. Phys. Chem. C*, 2013, **117**, 23908-23918.

5. T. W. Birky, J. T. Kozlowski and R. J. Davis, *J. Catal.*, 2013, **298**, 130-137.

6. A. K. P. Mann, Z. Wu, F. C. Calaza and S. H. Overbury, *ACS Catal.*, 2014, **4**, 2437-2448.